

## Coupling between High-Frequency Plasma Waves in Laser-Plasma Interactions

M. J. Everett, A. Lal, C. E. Clayton, W. B. Mori, T. W. Johnston,\* and C. Joshi

*Electrical Engineering Department, University of California Los Angeles, Los Angeles, California 90024*  
(Received 3 October 1994)

Experimental evidence for the coupling between two electron plasma waves having nearly the same frequency but greatly differing in wave number is presented using time and wave-number resolved spectra of Thomson scattered light from the plasma. The qualitative features of the measured  $w(t, k)$  spectra are predicted by a Lagrangian fluid description and reproduced in particle simulations. These show that the daughter waves generated in this mode coupling process take the energy preferentially from the large  $k$  wave without significantly affecting the small  $k$  plasma wave.

PACS numbers: 52.35.Mw, 52.40.Nk, 52.50.Jm

Waves in plasmas [1] is a major subtopic in the area of plasma physics. The nonlinear coupling between waves, although greatly investigated theoretically [2], remains relatively less explored in controlled laboratory experiments. In this Letter we show conclusive evidence for the coupling between two laser-excited electron plasma waves which have almost the same frequency but greatly different wave numbers. We find that the daughter waves generated in this process take the energy preferentially from the short wavelength wave while the long wavelength wave acts essentially as a catalyst. Besides being of fundamental interest, this coupling has implications for laser fusion and plasma accelerators.

As is well known, an unmagnetized plasma can support two types of longitudinal waves: ion acoustic waves and electron plasma waves. If simultaneously excited in a plasma, the low-frequency ion acoustic wave can couple a long wavelength but high-frequency plasma wave into shorter wavelength "quasimodes" via quasisonant mode coupling. The short wavelength quasimodes can be irreversibly damped by the resonant plasma particles (Landau damping), thus dissipating the energy of the original plasma wave [1,3]. Such mode coupling has been seen in laser-plasma experiments [4] and explained theoretically [3]. Here, using experimental data and supporting simulations, we demonstrate a different coupling, independent of ion motion, between two electron plasma waves having very different wave numbers.

The dispersion relation of an electron plasma wave ( $w, k$ ) in an unmagnetized plasma is given by  $w^2 = w_p^2 + 3k^2 v_{th}^2$ , where  $w_p$  is the plasma frequency and  $v_{th}$  is the thermal velocity of the plasma electrons. If the thermal correction to the plasma wave dispersion relation is small,  $w \approx w_p$ . Unlike coupling between ion acoustic and electron plasma waves [3], the mode coupling between two electron plasma waves generates modes at integer multiples of  $w_p$ . To understand this coupling at  $nw_p$ , we consider two electron plasma waves in a zero temperature plasma. Lagrangian coordinates are used because in these coordinates the two waves are separable. Relativistic corrections are higher order than the coupling ef-

fects and thus neglected in this derivation. The general position of an electron  $z$  is written as  $z = z_0 + \xi$ , where  $z_0$  is the initial electron position, and  $\xi = \xi_1 + \xi_2$  is the perturbation due to the two plasma waves. The restoring force on the electrons is  $-eE$ , where  $E = 4\pi en_0(\xi_1 + \xi_2)$  from Gauss' law. The equation of motion is then  $m\partial^2 z/\partial t^2 = -4\pi n_0 e^2(\xi_1 + \xi_2)$ , or  $\partial^2(\xi_1 + \xi_2)/\partial t^2 = -w_p^2(\xi_1 + \xi_2)$ . This is a simple harmonic oscillator equation with solutions that can be written as  $\xi_{1,2} = \epsilon_{1,2} \sin(\psi_{1,2})/k_{1,2}$ , where  $\epsilon_1$  and  $\epsilon_2$  are the dimensionless amplitudes ( $\delta n_{1,2}/n_0$ ) of the two waves in the Lagrangian frame,  $\psi_{1,2} = (k_{1,2}z_0 - w_{1,2}t)$ , and  $w_1 \approx w_2 \approx w_p$ . In the actual experiment  $w_1$  and  $w_2$  will not be exactly  $w_p$  because of thermal effects. The density perturbations can be calculated from the electron displacement using the equation

$$\frac{\tilde{n}(z)}{n_0} = \left( \frac{\partial z}{\partial z_0} \right)^{-1} = \frac{1}{1 + \epsilon_1 \cos(\psi_1) + \epsilon_2 \cos(\psi_2)}. \quad (1)$$

Lagrange's implicit function theorem can then be used to determine the density perturbations in the laboratory frame by eliminating  $z_0$  (contained in  $\psi_{1,2}$ ) in Eq. (1), resulting in the equation [5]

$$\frac{\tilde{n}(z)}{n_0} = \sum_{n=0}^{\infty} \frac{(-1)^n}{n!} \frac{\partial^n}{\partial z^n} [\xi_1(z, t) + \xi_2(z, t)]^n. \quad (2)$$

The effect of an electron wave with a small wave number  $k_2$  on a large wave number  $k_1$  wave can be seen by expanding this equation to third order under the assumption  $k_1 \gg k_2$  for  $\epsilon_2 k_1/2k_2 \ll 1$ :

$$\begin{aligned} \frac{\tilde{n}}{n_0} = & 1 - \epsilon_1 \left[ 1 - \left( \frac{\epsilon_2 k_1}{2k_2} \right)^2 \right] \cos(\psi_1) - \epsilon_2 \cos(\psi_2) \\ & - \epsilon_1 \left( \frac{\epsilon_2 k_1}{2k_2} \right) [\cos(\psi_1 - \psi_2) - \cos(\psi_1 + \psi_2)] \\ & - \frac{\epsilon_1}{2} \left( \frac{\epsilon_2 k_1}{2k_2} \right)^2 [\cos(\psi_1 - 2\psi_2) + \cos(\psi_1 + 2\psi_2)]. \quad (3) \end{aligned}$$

The phase velocity of a wave of a given frequency is inversely proportional to its wave number,  $v_{ph} = w/k$ . Since in the experiment  $v_{ph}(k_2) \approx c$ , whereas  $v_{ph}(k_1) \ll c$ , the small wave number  $k_2$  wave will be referred to as the

“fast wave” and the  $k_1$  wave as the “slow wave” throughout this Letter. Equation (3) indicates that unlike the harmonics of a single wave, which are typically small compared to the fundamental, the amplitudes of the coupled waves can be as large or larger than the slow wave if  $\epsilon_2 \approx 2k_2/k_1$ . Although Eqs. (2) and (3) break down in this case because the infinite series is nonconvergent, an iterative numerical solution to Eq. (1) shows that the coupled modes can be larger than the primary slow wave.

This amplitude for  $\epsilon_2$  can be very small: for instance,  $2k_2/k_1 \approx 3\%$  for fast waves from forward Raman or from beat excitation coupling to a slow wave from backward Raman in an underdense plasma of density  $n/n_{\text{crit}} \approx 10^{-3}$ . As is evident in Eq. (3), the amplitude of the slow wave is reduced by this coupling while the fast wave is unaffected. Physically, this is because the displacement of the electrons by the fast wave can be on the order of the wavelength of the slow waves, but the displacement of the electrons by the slow wave is negligible compared to the wavelength of the fast wave. The  $\cos(\psi_1 - \psi_2)$  term in Eq. (3), although not discussed in detail in this paper, may be important on the ion time scale as it has a frequency near zero and thus may transfer energy directly to ion acoustic waves. These ion acoustic waves can then further perturb the electron plasma waves, leading to the quasisonant mode coupling mentioned earlier.

To experimentally demonstrate the electron plasma wave coupling, we excite two electron plasma waves with a wave-number ratio  $k_1/k_2 = 70$ . This is done in the following manner: A short but intense laser pulse containing two frequencies ( $w_a, w_b$ ) is fired into a plasma such that the frequency difference is  $w_a - w_b \approx w_p$ . This resonantly excites a plasma oscillation through the process of collinear optical mixing with a relativistic phase velocity (fast wave) at the resonant frequency  $w_2 \approx w_p$  and wave number  $k_2 = k_a - k_b$ , the difference in the wave numbers of the two laser modes [6]. Two slow wave modes at  $(w_{1a}, k_{1a})$  and  $(w_{1b}, k_{1b})$  are also excited via a three wave parametric process, the stimulated Raman backscatter instability (SRS) [7], when the laser pulse exceeds the instability threshold. The wave numbers of these modes are close to twice the wave numbers of the two laser modes, i.e.,  $k_{1a,b} = 2k_{a,b} - w_p/c$ . There is little coupling between the two slow waves as they have similar wave numbers. However, the fast wave, with a  $k$  of  $\frac{1}{70}$  of the slow waves, strongly modifies the modal structure of the slow waves, generating daughter plasma modes at  $(w_{1a,b} \pm nw_2, k_{1a,b} \pm nk_2)$ .

In the experiment, where the fast and slow waves are driven by collinear optical mixing and SRS, respectively, the amplitudes of the daughter modes will be modified by coupling to both the laser and the ions. Although stimulated Brillouin scattering (SBS) [7] grows more slowly than the SRS, the SRS backscatter of the higher-frequency pump beats with the lower-frequency

pump, forcing the growth of a standing wave ion perturbation at wave number  $2k_b$ , twice the  $k$  of the lower-frequency laser line. This can seed SBS [8] on that laser line. The SRS instability at  $2k_b$  has approximately the same frequency and wave number as the slow (fast) wave coupling at  $w_{1a} - w_2 \approx 0$ ,  $k_{1a} - k_2 \approx 2k_b$ , and thus strongly perturbs this mode. This ion ripple can also affect the other plasma modes through electron (ion) wave coupling. Complicating the matter further, the modes near zero frequency may be ion or electron Landau damped. Thus we expect to reproduce, in the experiment, the frequency and wave-number spectra of the coupled modes only in a qualitative sense.

The experimental setup has been described in detail elsewhere [9]. Briefly, a CO<sub>2</sub> laser operating on two lines, 10.29 and 10.59  $\mu\text{m}$ , first creates the plasma by the tunneling ionization of static gas, 140 mTorr H<sub>2</sub>, and then drives the fast and slow plasma waves as discussed above. The laser has a peak intensity of about  $2 \times 10^{14}$  W/cm<sup>2</sup>, divided roughly equally between the two lines. The resonant plasma density is  $\approx 8.5 \times 10^{15}$  cm<sup>-3</sup>. The laser rise time is  $\approx 100$  ps and the pulse width is  $\approx 300$  ps FWHM. Collective Thomson scattering of a probe laser is used to measure the plasma density fluctuations associated with the slow wave and coupled waves. The incident angle of the 2 ns (FWHM), 50 MW, 0.53  $\mu\text{m}$  optical probe laser beam is chosen to  $k$  match to the  $k_{1a}$  Raman backscatter mode. The coupled slow waves ( $k_1 + nk_2$ ) also appear on the Thomson scattering diagnostic, but scatter less efficiently as they have a  $k$  mismatch relative to the probe laser of  $\approx nk_2$ . Thus, although both the primary Raman mode and coupled modes are visible on this diagnostic, it is difficult to make absolute comparisons of the relative amplitudes of the modes. To gain the maximum information about the modes, we resolve the frequency of scattered light in both time  $w(t)$ , using a spherically focused probe beam and a streak camera, and wave number  $w(k)$ , using a cylindrically focused probe beam [9,10]. By resolving the evolution of the frequency spectrum versus time, we distinguish between the electron waves and the ion-wave-related features which occur later in time. The  $w(k)$  resolved measurements, on the other hand, allow us to associate a wave number with each frequency and show the shift of  $(nw_2, nk_2)$  associated with coupling with the fast wave. The time resolved measurements have a time resolution of 20 ps and a  $w$  resolution of  $0.1w_p$ , while the  $k$  resolved data has a resolution of  $0.3w_p/c$  in wave number and  $0.3w_p$  in frequency.

Figure 1(a) shows the time resolved spectrum around  $k_1$  when a single wavelength (10.59  $\mu\text{m}$ ) laser beam is fired into the plasma. We clearly see a relatively narrow feature characteristic of strongly driven [7] SRS at  $w_p$  that lasts for 40 ps FWHM before evolving into a Compton spectrum [11]. Figure 1(b) shows the time resolved spectrum around  $k_2$  when a two frequency laser

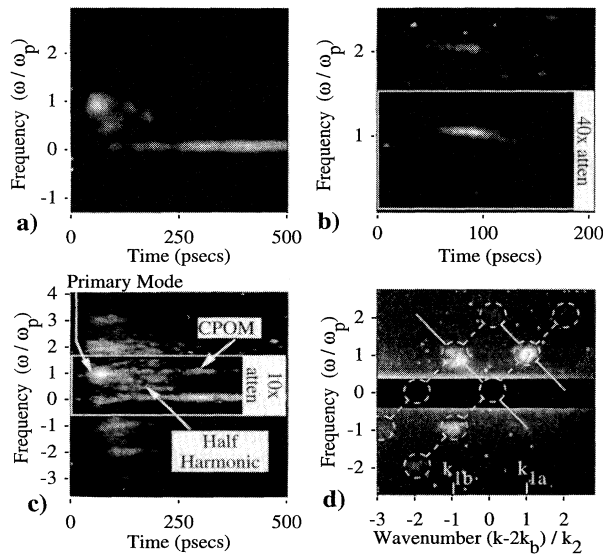


FIG. 1. Experimental results: (a) time resolved slow wave (Raman) spectrum, single frequency laser; (b) time resolved fast wave spectrum, two frequency laser; (c) time resolved slow wave spectrum, two frequency laser; and (d) coupled slow wave spectrum,  $(\omega, k)$  resolved, two frequency laser. Dotted lines connect circled Raman modes coupled by fast wave.

is fired into the resonant density plasma and excites the fast wave. The signal at  $w_p$  is the fast wave and that at  $2w_p$  is the second harmonic of the fast wave at wave number  $2k_p$ . The ratio of the two signals and their absolute levels indicate a peak fast wave amplitude of  $\approx 20\%$  [9]. Figure 1(c) shows the time resolved frequency spectrum around  $k_1$  (slow waves) when a dual frequency laser beam is fired into the plasma. In addition to the SRS modes from both lines appearing near  $w_p$ , one now sees a series of modes at  $w_1 + nw_2$ , where  $-4 \leq n \leq 2$ . The mode near zero frequency appears weak because of the  $10\times$  attenuator placed over the frequency range of  $-0.5w_p$  to  $1.5w_p$ . It is slightly below zero frequency, which is marked by the long tail of SBS extending beyond 500 ps, indicating that the Raman backscatter frequency  $w_1$  is slightly below the fast wave frequency  $w_2$ . This may be caused by Raman wave breaking [11] or growth of Raman before full tunneling ionization of the plasma has been obtained. The coupled modes appear rather broad because the Raman is in the strongly driven regime [7]. The coupled modes typically last for 40 to 75 ps FWHM as evidenced by the broad feature at  $w = 3w_p$ , in good agreement with the lifetime of the  $k_1$  mode at  $w = w_p$  and that of the  $k_2$  mode shown in Fig. 1(b). The peaks of the coupled modes occur after that of the Raman mode at  $w_p$ , an effect also seen in the simulations to be discussed later. This is consistent with Eq. (3) if one assumes that the fast wave is growing and thus coupling more energy from the Raman mode into the coupled modes later in time.

However, quantitative comparison between experiment and theory is not possible without a fully time dependent theory including ion effects. There is a narrow well-defined feature at  $w_p$  labeled as CPOM, which extends out to 350 ps from the broad primary  $k_1$  Raman mode. This is probably either a result of counterpropagating optical mixing (CPOM) or quasis resonant electron (ion) wave coupling [4]. In addition to these, we have often seen enhancement of scattering at about  $(1/2)w_p$ , which is as yet unexplained [12]. The feature at  $(1/2)w_p$  can be seen in Fig. 1(c) about 50 ps after the peak of the fast (slow) wave coupling.

That the coupled modes are indeed discrete in  $k$  space can be seen in the  $w(k)$  spectrum of the slow waves shown in Fig. 1(d). Here, the two primary modes due to Raman can be clearly seen near  $w_p$  and separated by  $2k_2$  as expected. The Raman mode due to  $10.59 \mu\text{m}$  in this particular example extends to frequencies somewhat below  $w_p$ . This is believed to be due to wave breaking of the oscillation and its evolution into Compton scattering [11]. This downshifting is also evident in the time resolved spectrum of the single frequency Raman shown in Fig. 1(a). Coupled modes at near zero frequency shift are not seen because they are under a mask which blocks the stray light. The positions of the expected coupled modes are shown by circles on the dotted lines. The dotted lines have a slope  $\partial w / \partial k = w_2 / k_2 = c$  and the coupled modes lie on these lines separated by  $(w_2, k_2)$ . The coupled modes of the  $10.29 \mu\text{m}$  Raman ( $k_{1a}$ ) at  $n = +1, -2$ , and  $-3$  ( $2w_p, -w_p$ , and  $-2w_p$ ) and that of the  $10.59 \mu\text{m}$  ( $k_{1b}$ ) Raman at  $n = +1$  and  $-2$  ( $2w_p$  and  $-w_p$ ) are clearly visible.

These results were reproduced with 1D electromagnetic particle-in-cell (PIC) simulations using the code WAVE [13]. To show the theoretically predicted coupling between plasmons of widely differing  $k$ 's without the complications of the two laser pulses, plasmons at wave numbers  $k_1$  and  $k_2$  were excited at a frequency  $w_p$ , using periodic longitudinal forces of the form  $F = F_1 + F_2$ , where  $F_{1,2} = (0.005/k_{1,2}) \sin(w_p t - k_{1,2} x)$  and  $k_1 = 10w_p/c$ ,  $k_2 = 1w_p/c$  are the slow and fast waves, respectively. The ions were immobile and  $k_1 \lambda_D$  was 0.1. The temporal evolution of the frequency spectra of the electrostatic modes near  $k_1$  and  $k_2$  are shown in Figs. 2(a) and 2(b), respectively. The spectrum near  $k_2$  includes both the fundamental and second harmonic of the fast wave as also seen in the experimental data in Fig. 1(b). In Fig. 2(a), the growth of the initial wave at  $(w_1 \approx w_p, k_1)$  occurs first, quickly followed by coupled modes at  $w_p + nw_p$ . These correspond to the coupled modes at  $(w_1 + nw_2, k_1 + nk_2)$  which are seen in the experimental results in Figs. 1(c) and 1(d). The time evolution of the amplitudes of the driven modes ( $k_1$  and  $k_2$ ) and the coupled modes is shown in Fig. 2(c). Lines (1) and (2) show the growth of the fast and slow wave, respectively, when the other wave is not present, i.e., when only  $F_1$  or  $F_2$  is

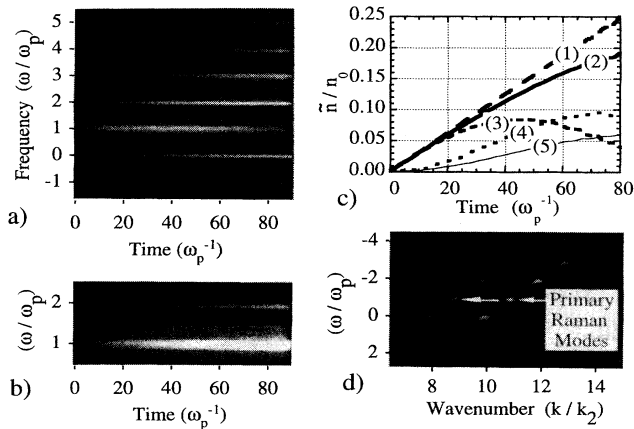


FIG. 2. PIC simulations showing coupling of slow and fast electron plasma waves. Results from the  $F_{1,2}$  driver are shown in (a)–(c). Spectrum of the density perturbation ( $\tilde{n}/n_0$ ) vs time for modes near (a)  $k_1$  and (b)  $k_2$ . (c) Time histories of particular modes: (1) Fast wave ( $k_2$ ) whether or not slow wave ( $k_1$ ) is driven. (2) Slow wave if fast wave is not driven. (3) Slow wave if fast wave is driven. (4) and (5) coupled modes at ( $2w_p, k_1 + k_2$ ) and ( $0w_p, k_1 - k_2$ ), respectively. Curves (3)–(5) are taken from (b). (d) Time integrated ( $w, k$ ) spectrum ( $\tilde{n}/n_0$ ) of the coupling between Raman waves and a beat-excited fast wave.

applied to the plasma. The waves initially have a secular growth rate of  $0.005w_p^{-1}/2$ , as expected from a resonantly driven oscillator [6]. The growth rate of the slow wave decreases over time because of the frequency mismatch between the driving frequency  $w_p$  and the natural Bohm-Gross frequency  $w$  of this mode. As expected from Eq. (3), the fast ( $k_2$ ) wave is unaffected by the presence of the slow wave and thus the growth of the fast wave in the presence of the slow wave is also given by line (1). Lines (3)–(5) show the evolution of the primary and coupled slow waves when both the fast and slow waves are driven. As expected from Eq. (3), the amplitude of the slow wave ( $k_1$ ) is greatly reduced by the presence of the fast wave. The externally driven slow wave grows and saturates around  $40w_p^{-1}$  at  $\tilde{n}/n_0$  of  $\approx 8\%$  and actually begins to decrease thereafter. The coupled modes at ( $w_1 - w_2 \approx 0w_p, k_1 - k_2$ ) and ( $w_1 + w_2 \approx 2w_p, k_1 + k_2$ ) in fact grow to a larger amplitude than the driven mode at ( $w_1, k_1$ ) by the end of the simulation. The mode at ( $\approx 0w_p, k_1 - k_2$ ) could be ion Landau damped if the simulation included mobile ions, irreversibly thermalizing the coherent motion of the electrons that participate in this mode. Not only does the presence of the fast wave transfer energy to the coupled waves, it also reduces the excitation of the slow wave by the external driving force. This is made clear by comparing the total energy in all the coupled slow waves,

proportional to  $\sum[\tilde{n}(w, k)/kn_0]^2$ , to that of the unperturbed slow wave. The total energy is reduced by  $\approx 40\%$  at time  $80w_p^{-1}$ .

Finally, we have reproduced the ( $w, k$ ) spectrum measured in the experiment in a fully self-consistent 1D PIC simulation by replacing the forces  $F_1$  and  $F_2$  in the wave simulations with two concurrent  $300w_p^{-1}$  rise-time electromagnetic waves (laser pulses) with frequencies of  $5w_p$  and  $6w_p$  and peak amplitudes of  $v_{osc}/c = 0.1$ . Just as in the experiment, the Raman instability (slow wave) grows from noise at ( $w_p, k_{1,a,b}$ ), where  $k_{1,a,b} = 2k_{a,b} - k_p = 9k_p, 11k_p$  ( $k_p = w_p/c$ ), and the fast wave is driven by collinear mixing at ( $w_p, k_p$ ). The ( $w, k$ ) spectrum of the slow waves time integrated from 0 to  $300w_p^{-1}$  is given in Fig. 2(d), showing the coupling of the slow waves to the fast wave at ( $w_p + nw_p, k_{1,a,b} + nk_p$ ) just as in the experimental ( $w, k$ ) spectrum shown in Fig. 1(d).

In conclusion, the coupling between laser-excited high-frequency electron plasma waves having similar frequencies but greatly differing in wave number has been seen in experiments and explained. This process couples energy from the large wave-number, low phase velocity plasma wave ( $w_1, k_1$ ) to a manifold of waves at ( $w_1 \pm nw_2, k_1 \pm nk_2$ ) without significantly affecting the small wave-number, high phase velocity plasma wave ( $w_2, k_2$ ), as shown by a Lagrangian fluid description and verified using PIC simulations.

This work was supported by DOE Grant No. DE-AS03-83-ER40120. We thank D. Gordon and K. Marsh for their help in this work.

\*Also at Institut National de La Recherche Scientifique-Energie, Quebec, Canada.

- [1] N. A. Krall and A. W. Trivelpiece, *Principles of Plasma Physics* (San Francisco Press, Inc., CA, 1986); T. H. Stix, *The Theory of Plasma Waves* (McGraw-Hill, New York, 1962).
- [2] R. C. Davidson, *Methods in Nonlinear Plasma Theory* (Academic Press, New York, 1972).
- [3] P. K. Kaw *et al.*, Phys. Fluids **16**, 1967 (1973).
- [4] C. Darrow *et al.*, Phys. Rev. Lett. **56**, 2629 (1986).
- [5] E. A. Jackson, Phys. Fluids **3**, 831 (1960).
- [6] M. N. Rosenbluth and C. Liu, Phys. Rev. Lett. **29**, 701 (1972).
- [7] D. W. Forslund *et al.*, Phys. Fluids **18**, 1002 (1975).
- [8] H. E. Huey *et al.*, Phys. Rev. Lett. **45**, 795 (1980).
- [9] M. J. Everett *et al.* (to be published).
- [10] D. M. Villeneuve *et al.*, J. Opt. Soc. Am. B **8**, 895 (1991).
- [11] M. J. Everett *et al.*, Phys. Rev. Lett. **74**, 1355 (1995).
- [12] W. P. Leemans *et al.*, Phys. Rev. A **46**, 5112 (1992).
- [13] R. L. Morse and C. W. Nielson, Phys. Fluids **14**, 830 (1971).

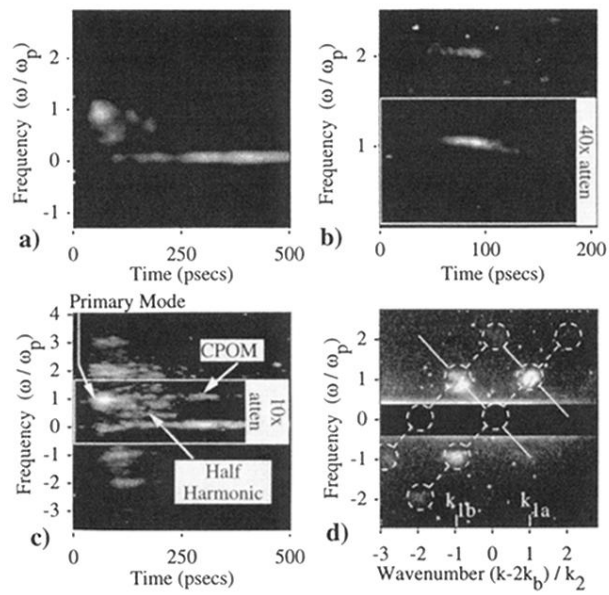


FIG. 1. Experimental results: (a) time resolved slow wave (Raman) spectrum, single frequency laser; (b) time resolved fast wave spectrum, two frequency laser; (c) time resolved slow wave spectrum, two frequency laser; and (d) coupled slow wave spectrum,  $(\omega, k)$  resolved, two frequency laser. Dotted lines connect circled Raman modes coupled by fast wave.

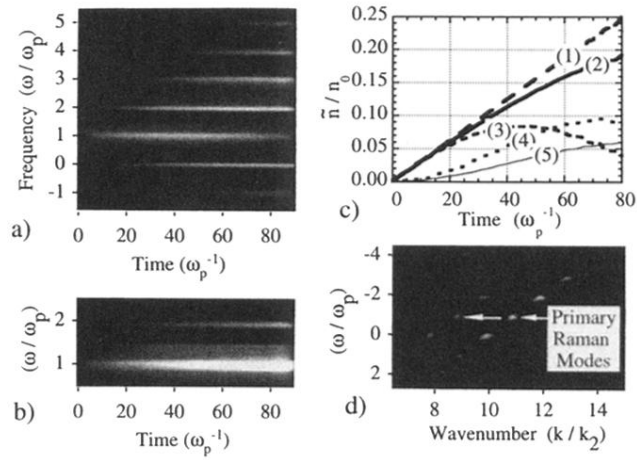


FIG. 2. PIC simulations showing coupling of slow and fast electron plasma waves. Results from the  $F_{1,2}$  driver are shown in (a)–(c). Spectrum of the density perturbation ( $\tilde{n}/n_0$ ) vs time for modes near (a)  $k_1$  and (b)  $k_2$ . (c) Time histories of particular modes: (1) Fast wave ( $k_2$ ) whether or not slow wave ( $k_1$ ) is driven. (2) Slow wave if fast wave is not driven. (3) Slow wave if fast wave is driven. (4) and (5) coupled modes at  $(2\omega_p, k_1 + k_2)$  and  $(0\omega_p, k_1 - k_2)$ , respectively. Curves (3)–(5) are taken from (b). (d) Time integrated  $(\omega, k)$  spectrum ( $\tilde{n}/n_0$ ) of the coupling between Raman waves and a beat-excited fast wave.